processes

MDPI

Article

Application of a Multi-Objective Optimisation (MOO) via Pareto Front to the Energy Performance of a Domestic Oven

Simona Rustico [1,*], Beatrice Bonfanti Pulvirenti [1] and Marco Reguzzoni [2]

[1] Department of Industrial Engineering (DIN), Alma Mater Studiorum Università di Bologna, Viale Risorgimento 2, 40136 Bologna, Italy; beatrice.pulvirenti@unibo.it
[2] Research and Development Department, SMEG S.p.A., Via Leonardo da Vinci 4, 42016 Guastalla, Italy; marco.reguzzoni@smeg.it
* Correspondence: simona.rustico2@unibo.it

Abstract

The growing demand for environmentally sustainable technologies is driving the adoption of increasingly stringent energy regulations across Europe. The residential sector is particularly impacted, not only through requirements for highly insulated buildings but also through stricter standards for household appliances. Among these, domestic ovens represent a critical target, requiring manufacturers to develop technologies that support laboratory testing while reducing energy consumption. This work proposes a tool to support manufacturers during laboratory testing by applying a multi-objective optimisation approach using the Pareto front method. The code was developed in MATLAB® and aims to minimise final consumption by acting exclusively on the management of the heating element. The results obtained from the code are first tested in the Simulink® digital model of the oven and then through experimental testing. The results demonstrate that the proposed tool, specifically tailored for these systems, provides outcomes consistent with real operating conditions, while enabling a substantial reduction in laboratory testing time.

Keywords: multi-objective optimisation; Pareto front; energy consumption

1. Introduction

According to Eurostat, most of the EU's final energy consumption in the residential sector is covered by electricity (24.6%). Household appliances represent the most significant source of consumption. This awareness emphasises the development of more effective technologies to minimise energy consumption. European standards on the energy consumption of ovens standardise the techniques for classifying the energy efficiency of these appliances. Due to regulatory requirements, companies have invested resources in research to develop new technologies aimed at reducing consumption. These new technologies, such as pulsed electric fields (PEF) [1], ohmic heating [2], are very promising techniques. However, they almost never reached the market due to relative technological issues (e.g., production cost). For this reason, while many researchers are focusing on new technologies, others are more interested in optimising processing using consolidated technologies [3]. For example, this includes quantifying the energy demand for food and the process-related energy consumption, allowing optimisation of the total energy absorbed by the product [4]. The numerical approach is certainly widespread among the various methods, and dynamic models are essential tools for design and control. Usually, a lumped-parameter-based methodology is considered to develop a low-order dynamic model, reducing computational cost and

Academic Editors: Md Rasheduzzaman and Yongming Han

Received: 18 February 2026
Revised: 16 March 2026
Accepted: 17 March 2026
Published: 19 March 2026

run-time [5–7]. In these works, an analysis of energy consumption was carried out in accordance with EN 60350 [8]. By implementing a brick model and adopting alternative formulations of the evaporation term, we lay the foundation for the development of an accurate numerical model. In one approach, evaporation was modelled through a linear relationship between oven temperature and load temperature [6], while in another, it was expressed as a function of vapour pressure, which depends on the temperature measured at the brick surface [7]. In this type of system, energy consumption is typically associated with the oven's heating elements. Further studies focused on the product's energy demand, accounting for sensible and latent heat contributions [9]. A more detailed analysis was carried out by examining the heater usage algorithm governing the cooking process in a domestic oven. Numerical simulations and experimental tests were performed to examine heat distribution and the primary mechanisms of heat loss. The fidelity of the baking-process model was further improved by modelling evaporation and condensation phenomena within the thermal properties of a cupcake [10]. Among the various optimisation techniques, the multi-objective technique is also included as an algorithm aimed at reducing energy consumption. These studies represent the largest category (47%) and are most frequently implemented using MATLAB (32%) [11]. Multi-objective optimisation turns out to be a very useful tool for critical challenges in advanced energy systems, such as thermal energy storage devices based on phase change materials and heat exchangers, where optimisation strategies are used to simultaneously improve heat transfer and system efficiency [12]. Similarly, hybrid methodologies combining Computational Fluid Dynamics and Design of Experiments have been employed to identify optimal operating conditions for industrial equipment, such as centrifugal fans used in industrial ovens [13]. Furthermore, it is used to achieve cleaner, more sustainable systems, thereby reducing CO_2 emissions [14]. Moreover, this method can be used to develop a model based on active power losses and voltage deviation. Within the food and cooking sector, optimisation frameworks have been adopted to improve thermal processes and product quality. For instance, model-based multi-objective optimisation has been applied to beef roasting to balance energy consumption, cooking time, and final product characteristics [15]. In addition, multi-objective optimisation frameworks have been proposed for energy management in commercial baking processes to simultaneously optimise energy use and thermal performance during bread baking [16]. Within this framework, the Pareto front serves as the solution tool for the multi-objective optimisation problem [17]. However, they are also used to identify the optimal locations for installing power-quality monitors, aiming to minimise investment costs while ensuring adequate observability of power-quality disturbances, particularly voltage sags [18]. The variety of available multi-objective optimisation algorithms continues to expand. Recent studies have extended these methods to complex mechanical systems, such as six-axis manipulators, to simultaneously optimise motion paths and control energy consumption [19]. The use of the Pareto front and its variants remains a widely explored topic in the literature, with studies focusing on adapting these algorithms to a broad range of engineering applications [13,20–23]. Multi-objective optimisation methods are frequently employed in thermal and energy systems to negotiate conflicting goals, including efficiency, cost, and performance. Most research focuses on temperature uniformity or component design rather than on reducing electrical energy use; therefore, their application to domestic cooking appliances is limited. Using the Pareto front approach, this study develops a multi-objective optimisation framework and applies it to the thermal control of a heating cavity system typical of a domestic oven. Using a multi-objective approach with a physics-based digital model, the method reduces energy and time demands, thereby enabling the discovery of optimal operating settings. First examined with the dynamic model created in MATLAB/Simulink (version R2024a, MathWorks), results are then verified via lab experiments.

2. Digital Model

A digital model of the system, namely a physical model that reproduces the dynamics of the real system and its interactions with the environment, is needed to test the control strategy and compare it with the real system. In this section, the oven considered in this analysis is presented, and a brief description is given of the approach used for modelling the different components, with a special emphasis on the control system.

2.1. System Description

The system considered is an electromechanical domestic oven with a volume of 70 L. The oven has an enamelled steel outer shell designed to withstand high temperatures. The front section includes a door fitted with low-emissivity, double-layer tempered glass to ensure both thermal insulation and user safety. The cooking chamber is coated with nonstick materials and equipped with support guides for racks and drip pans. Heating is provided by electric elements positioned at the top and bottom of the cavity. Figure 1 shows the dimensions and the main components of the oven. Two heating elements, called Grill and Cielo, are mounted on the upper wall of the cavity. The bottom element, called Suola, is located in a drawer below the cooking chamber. A fan, covered by a baffle, is mounted on the rear wall, allowing forced-convection operation during ventilated cooking modes. The baffle has vents used to recirculate the air inside the cavity. The lateral walls (left and right), the back wall, the bottom surface, and the door define the thermal boundaries of the cavity. This configuration supports natural convection (static mode) and forced convection (ventilated mode), depending on the selected operating condition.

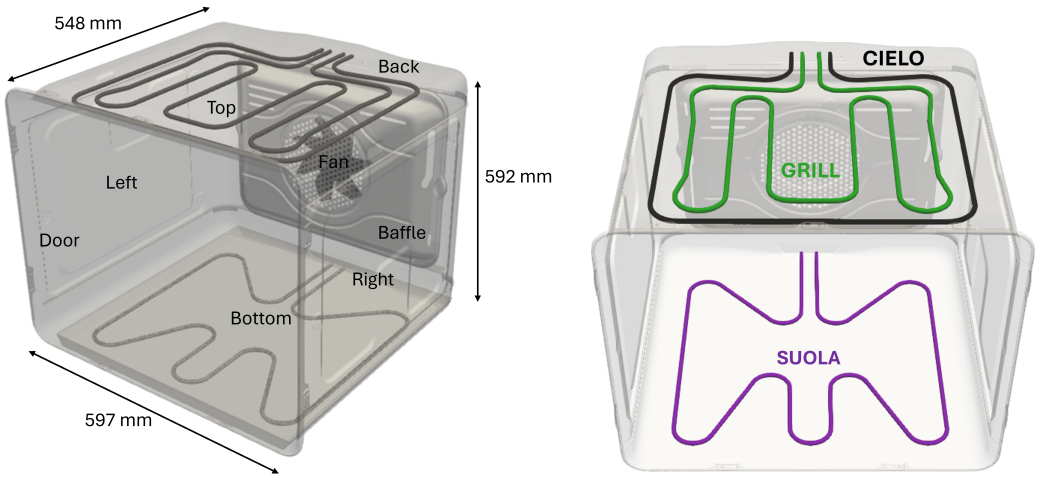

Figure 1. Overview of the oven considered in this analysis: (**a**) Names of the boundaries and the dimensions of the cavity walls; (**b**) Names of the three heating elements present in this model and their placement.

The control panel is equipped with three knobs:

- Temperature selector: regulates the oven temperature from 50 °C to 250 °C.
- Cooking function selector: allows the user to choose among several operating modes, including Static, Ventilated, Grill, and Eco.
- Timer: sets the desired cooking duration.

The digital model was developed in the MATLAB/Simulink environment and is based on a set of non-linear equations that describe the dominant heat-transfer mechanisms in the oven. It adopts a lumped-parameter formulation, detailed in a previous work [24].

In Table 1, all the nodes are listed and described. The energy balance for each node is expressed by:

$$C_i \frac{dT_i}{d\tau} = \sum_j Q_{conv\,i,j} + \sum_j Q_{rad\,i,j} + P_{el,i} + Q_{loss,i}, \quad (1)$$

where $P_{el\,i}$ represents the heat source term, which is non-zero only for the nodes corresponding to the heating elements. The oven walls are represented using thermal-block components, allowing the thermal properties of each layer to be specified. Convective, conductive, and radiative heat exchanges are implemented through dedicated physical blocks, each based on its corresponding physical laws and connections. As mentioned in [24], the heat transfer coefficients obtained from CFD analysis under steady state conditions are used as input in the dynamic model. The heating elements are described as a volume energy source, with an emissivity of 0.85 [25,26]. The interior elements, oven cavity, and baffle are prescribed with an emissivity of 0.9 [25–27]. The parameters do not depend on the temperature.

Table 1. Nodes considered for the lumped parameter model.

Nodes	$Q_{conv\,i,j}$	$Q_{rad\,i,j}$	$P_{el\,i}$	$Q_{loss\,i}$
Oven Cavity air (OC)	CW, GH and Brick	-	-	-
Grill heater (GH)	OC	CW and Brick	$P_{el,GH}$	-
Cavity walls (CW)	OC	CW and GH	-	$Q_{loss,CW}$
Bottom wall (BW)	OC and AIR BH	CW, BH, GH, BOW, and Brick	-	$Q_{loss,BW}$
Bottom heater (BH)	AIR BH	BW and BOW	$P_{el,BH}$	-
Bottom case wall (BOW)	AIR BH	BW and AIR BH	-	-

The dynamic system also incorporates a brick model to evaluate energy consumption in accordance with the standard [8]. The standard explains how to carry out the test in laboratories. The brick undergoes a preparation phase: it is soaked in cold water with two thermocouples inserted into the brick's core. Once it reaches approximately 5 °C, it is positioned on a rack in the centre of the oven. During the test, the sensor's temperature, the Brick's core temperature, and consumption are monitored. The test ends when the brick reaches +55 K. In the dynamic model, the brick is defined by two nodes, one associated with the external part BrS Equation (2) and one associated with the internal part BrC Equation (3) of the brick. According to [7] the relationship is defined as:

$$r(m_{dry}c_{dry} + m_w c_w)\frac{dT_{BrS}}{d\tau} = Q_{OCBrS} + Q_{BrCBrS} + Q^{rad}_{THBrS} + Q^{rad}_{TWBrS} + Q^{rad}_{BWBrS} + Q^{rad}_{RWBrS} + Q^{rad}_{LWBrS} + Q^{rad}_{BaBrS} + Q^{rad}_{DBrS} - \dot{m}_w \Delta h_{lv}, \quad (2)$$

$$\left[(1-r)(m_{\mathrm{dry}}c_{\mathrm{dry}} + m_w c_w) - m_{w\,ev}\,c_w\right]\frac{dT_{\mathrm{BrC}}}{dt} = Q_{BrC\,BrS}. \quad (3)$$

In this configuration, radiative heat transfer constitutes the dominant mechanism between the oven cavity and the brick surface. Additionally, evaporation plays a significant role during the heating phase and must be accounted for in the thermal modelling.

2.2. Electromechanical Control

Temperature control in an electromechanical oven is via a mechanical thermostat that regulates the heating elements. This liquid-expanding thermostat senses the temperature and turns the heating on and off. A thermometer bulb filled with heat-expanding fluid is placed in the cooking chamber. The bulb is connected to a capillary tube filled with the same fluid, which reaches the thermostat. As the temperature rises, the fluid in the

bulb expands, exerting pressure on a diaphragm in the thermostat. This pressure actuates an electrical contact, interrupting or reactivating the resistance circuit. The bulb in the dynamic model is represented as follows:

$$C_{bu}\frac{dT_{bu}}{d\tau} = \dot{Q}_{ocbu} + \dot{Q}_{TWbu} + \dot{Q}^{rad}_{TWbu} + \dot{Q}^{rad}_{THbu}. \quad (4)$$

The thermostat regulates the switching on and off of the heating elements. When the temperature drops below the set value, the thermostat closes the circuit and energises the heating elements. When the temperature is reached, the thermostat opens the circuit, cutting off the power. Temperature control is carried out in a cyclic on–off mode: the oven alternates between active heating phases and turning off the heating elements to maintain the desired temperature. The cycle does not maintain a perfectly constant temperature but fluctuates around the set value by about ±5 °C. A logic block represented the on/off behaviour of the resistors, which was called the switch. This has three inputs and one output:

- Threshold: a scalar signal or constant that determines the selection criterion.
- First option: the signal that will be routed if the condition is true.
- Second option: the signal that will be routed if the condition is false.
- Output: the signal selected according to the condition set.

The threshold input is calculated as the difference between the set-point temperature and the probe's temperature. If the measured temperature is below the set threshold, the thermostat closes the circuit and the heating elements start heating. When the temperature reaches the set value, the thermostat opens the circuit and turns off the heating elements. A gain block is used to express the power of each heater. The output is then used as input to a controlled heat flow that feeds the heating elements, modelled using a thermal block. Given that the goal is to determine the configuration that achieves minimal energy consumption, it is necessary to evaluate all possible combinations of the heating elements. In the experimental tests, we manually evaluated the operation of the heating elements in series and parallel configurations to assess the response of the electromechanical control system. Each setup was created by connecting the resistances based on the chosen circuit design and then operating the thermostat as described. In the series setup, the heating elements were powered one after another, with the thermostat managing the total circuit. This allowed the observation of the combined effect on the chamber temperature. In the parallel configuration, the elements were energised simultaneously, and the thermostat regulated their combined output, enabling the comparison of the temperature rise and the stability between the two setups. Figure 2 shows all the possible combinations implemented in the oven: in red, the parallel function, and in blue, the series function. During these manual tests, the oven's temperature cycles were monitored with the sensor bulb, confirming the expected on/off behaviour of the heating elements and the ±5 °C fluctuations around the set point. These tests validated the model assumptions and the logic implemented in the switch and gain blocks, ensuring that the digital representation of the heating control accurately reproduces the actual electromechanical behaviour for both series and parallel configurations.

The configurations considered in this study are representative of standard household electric oven architectures. Commercial appliances of this type are designed and certified according to internationally harmonised safety standards (IEC60335-2-6 [28] for stationary electric cooking ranges and ovens), which address electrical insulation, protection against electric shock, surface temperature limits, and mechanical safety. While the present work focuses on the modelling and optimisation of thermal performance, any practical implementation or deployment in a commercial product would require compliance with these safety standards by components and configurations.

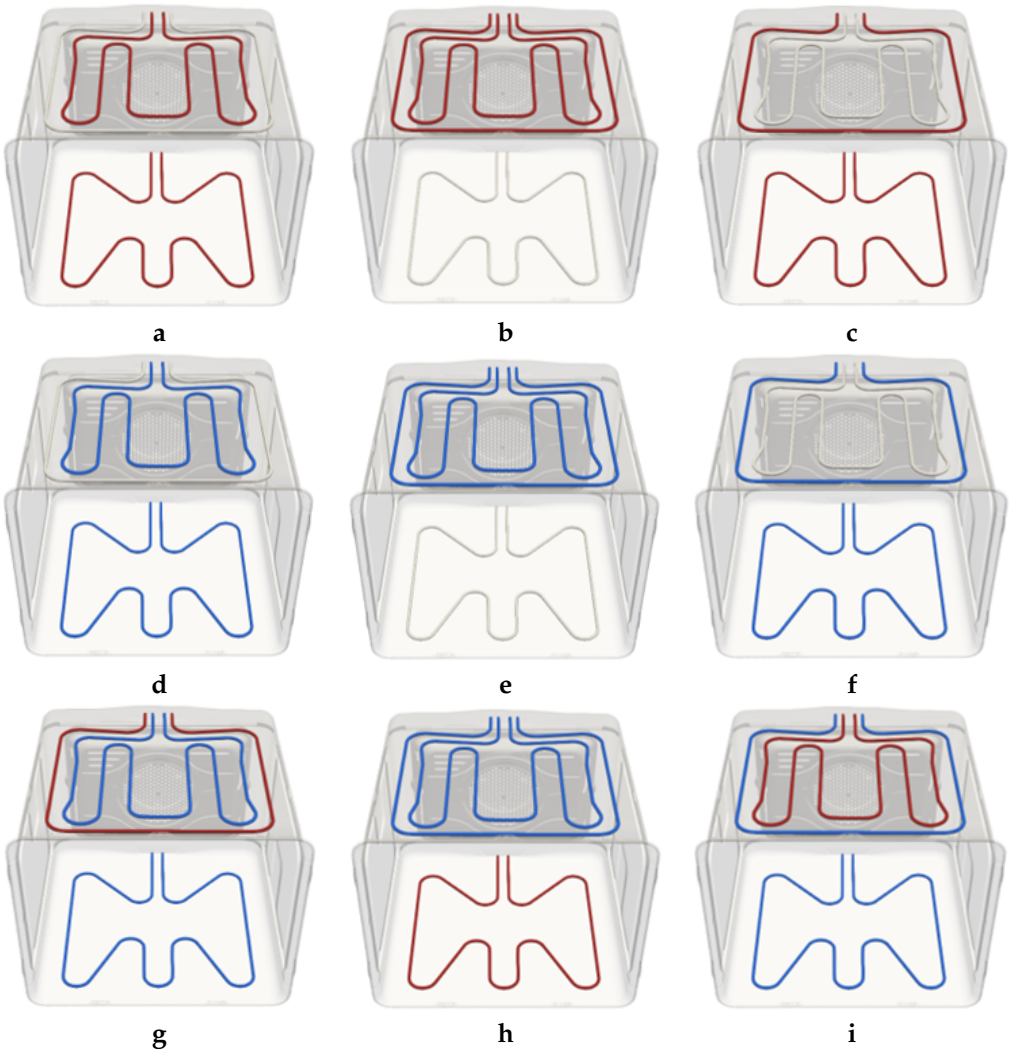

Figure 2. All the possible combinations implemented in the oven. In red: the parallel connection; in blue: the series connection. (**a**) Grill and Suola in parallel; (**b**) Grill and Cielo in parallel; (**c**) Suola and Cielo in parallel, (**d**) Grill and Suola in series; (**e**) Grill and Cielo in series; (**f**) Suola and Cielo in series; (**g**) Grill and Suola in series, with Cielo in parallel; (**h**) Grill and Cielo in series, with Suola in parallel; (**i**) Suola and Cielo in series, with Grill in parallel.

3. Optimisation Strategy

The approach used to achieve a lower energy consumption than the baseline relies on managing the power supplied to the heating elements. The standard operating mode plays the most significant role in determining the oven's energy class. According to the production standard, the grill element and the bottom heating element operate in parallel. The study began by identifying all possible heater configurations, in series and in parallel, available within the oven's electrical layout. As mentioned in Section 2.2, testing each configuration requires technicians to manually modify the wiring connections between heating elements. This procedure is not only labour-intensive but also time-consuming, as every wiring adjustment must be followed by a complete energy consumption measurement.

3.1. Generation and Power Constrained Selection of Heating Element Configurations

The first step in the optimisation process was the development of an initial script to compute all possible combinations of heating element configurations. Each electrical resistance is defined and associated with its nominal power rating (in watts). The code then generates all feasible combinations of heaters operating simultaneously. A for loop is

used in conjunction with the nchoosek function to produce every combination involving two or more resistors. For each resulting configuration, the corresponding power output is calculated. In parallel configurations, the total power is simply the sum of the individual resistor powers. In series configurations—applicable only to pairs of heaters—the total power is computed using the appropriate electrical relationship for series circuits:

$$\frac{(x \cdot y)}{(x + y)}, \tag{5}$$

where x and y are two generic power heaters. With an if loop, the constraint on the maximum acceptable power is applied. Only configurations with power <3000 W are accepted. The same process is carried out for the calculation of "mixed" combinations, i.e., those involving the resistors in series and one in parallel. Combinations of three active resistors are iterated to calculate all possible mixed connections. Finally, with an fprint, the valid combinations are printed, specifying the type: Parallel, Series, or Series + Parallel.

3.2. Development of the Thermal Model for Oven Performance Evaluation

The second part of the code set up a model for the oven's thermal behaviour. Table 2 shows all the parameters defined in the code.

Table 2. Thermal properties and operating parameters set for modelling the system's thermal behaviour.

Parameters	Value	Unit
Oven volume	70	L
Brick mass	2	kg
Brick heat capacity	2263.66	J/kg °C
Brick initial temperature	5	°C
Oven initial temperature	23	°C
Brick target temperature	+55 °C	°C
Efficiency heaters	0.7	-

Most model parameters were derived from the manufacturer, reference standards, and physical property correlations. Experimental tests were therefore used only for model validation, ensuring that the assessment of the model performance is independent from the parameter identification process and avoiding circular validation. The volume of the oven and the brick mass obtained from the datasheet. The brick heat capacity was calculated using the standard volume-based mixing rule:

$$c_s = \varphi_w c_w + (1 - \varphi_w) c_{b,dry}. \tag{6}$$

The initial and target temperatures for the brick and the oven were defined in accordance with the relevant reference standards. The efficiency of the heating elements was calculated as the ratio between the energy used for water evaporation and the total electrical energy supplied during the simulation. The heater combinations generated by the initial script are imported into this second code for further optimisation. A for loop is then executed, and for each valid configuration, it computes the energy and time required to heat the oven, transfer thermal energy to the brick, and produce the resulting temperature increase within the brick.

Polynomial Fitting of the Oven–Brick Thermal Transfer Function

To obtain the most realistic possible model of brick heating, the code incorporates a function that defines the relationship between the brick and oven temperatures. This

relationship is nonlinear and was derived experimentally through laboratory testing. The experiment was conducted under the production-standard operating mode, meaning the Grill and Suola in parallel. The brick was prepared according to the reference procedure explained in Section 2.1. During the test, the brick's core temperature and the oven temperature were continuously monitored using thermocouples. The measured data showed that heat transfer to the brick is nonlinear and can be accurately represented by a 4th-degree polynomial. The data obtained from the experiment were then processed using a dedicated script to derive the correlation. To quantify the relationship between the two data sets, the Pearson correlation coefficient was used [29], defined as follows:

$$r = \frac{Cov(X,Y)}{\sigma_X \cdot \sigma_Y}, \tag{7}$$

where:

$$Cov(X,Y) = \frac{1}{n}\sum_{i=1}^{n}(x_i - \bar{x})(y_i - \bar{y}), \tag{8}$$

$$\sigma_X = \sqrt{\frac{1}{n}\sum_{i=1}^{n}(x_i - \bar{x})^2}, \tag{9}$$

$$\sigma_Y = \sqrt{\frac{1}{n}\sum_{i=1}^{n}(y_i - \bar{y})^2}. \tag{10}$$

The polyfit function was used to determine the polynomial coefficients and the display command was used to visualise them.

3.3. Pareto Front-Based Multi-Objective Optimisation Computation

The optimisation method described in this work is based on a fundamental concept of multiobjective optimisation (MOO). The goal of MO optimisation is to find a set of acceptable solutions and present them to the Decision Maker, who will then choose among them. Additional constraints or criteria specified before or after the search by the DM can help guide, refine, or narrow the search [30]. The general MO optimisation problem requiring the optimisation of N objectives can be formulated as follows:

$$Minimize \quad \vec{y} = \vec{F}(\vec{x}) = [f_1(\vec{x}), f_2(\vec{x}), \ldots, f_N(\vec{x})]^T, \tag{11}$$

$$Subject\ to \quad g_j(\vec{x}) \leq 0, j = 1, 2, \ldots, M, \tag{12}$$

$$Where \quad \vec{x} = [x_1, x_2, \ldots, x_p]^T \quad \in \Omega, \tag{13}$$

$\vec{y}$ is the objective vector, g_j represents the constraints, and $\vec{x}$ is a P-dimensional vector representing the decision variables within a parameter space Ω. The space spanned by the objective vectors is called the objective space. The subspace of the objective vectors that satisfies the constraints is called the feasible space. To compare candidate solutions to the MO optimisation problems, the concepts of Pareto dominance and Pareto optimality are commonly used [31]. A solution belongs to the Pareto set if there is no other solution that can improve at least one objective without degrading any other objective. A decision vector $\vec{u} = [u_1, u_2, \ldots, u_p]^T$ is said to *Pareto-dominate* the decision vector $\vec{v} = [v_1, v_2, \ldots, v_p]^T$ in a minimisation context if and only if:

$$\begin{aligned} &\forall i \in 1, \ldots N, f_i(\vec{u}) \leq f_i(\vec{v}), \\ &and\ \exists j \in 1, \ldots N : f_j(\vec{u}) < f_j(\vec{v}). \end{aligned} \tag{14}$$

In the context of MO, Pareto dominance is used to compare and rank decision vectors: $\vec{u}$ dominates $\vec{v}$ in the Pareto sense means that $\vec{F}(\vec{u})$ is better than $\vec{F}(\vec{v})$ for all objectives, and there is at least one objective function for which $\vec{F}(\vec{u})$ is strictly better than $\vec{F}(\vec{v})$. A solution $\vec{a}$ is said to be Pareto optimal if and only if there does not exist another solution that dominates it. The corresponding objective vector $\vec{F}(\vec{a})$ is called a Pareto dominant vector or a non-inferior or non-dominated vector. The set of all Pareto optimal solutions is called the Pareto optimal set. The corresponding objective vectors are said to be on the Pareto front. It is generally impossible to come up with an analytical expression of the Pareto front. There are several approaches to solving multi-objective optimisation problems. The first is the weighted sum method, in which objectives are combined into a single scalar function. The function is represented by positive weights assigned to the objectives. Then there is the ϵ-binned objective function method. In this case, one objective is chosen to be optimised, and the others are transformed into constraints. Finally, there are multi-objective evolutionary algorithms, among them are NSGA-II (Non-dominated Sorting Genetic Algorithm) or MOEA/D (Multi-Objective Evolutionary Algorithm based on Decomposition). Unlike the first two, these explore the entire solution space by finding Pareto-efficient solutions without requiring explicit weights. The NSGA-II is one of the algorithms implemented in MATLAB via the gamultiobj function [32]. In general, it classifies solutions according to their dominance using generic operators such as selection, crossover, and mutation to explore the solution space and uses Crowding distance to maintain the diversity of solutions on the frontier. For this analysis, none of the built-in MATLAB fitting functions were used; instead, a dedicated, ad-hoc function was developed to address the problem's characteristics. The function was expressed as isPareto = computeParetoFront(data), where data represents the input, a matrix $N \times M$ where N is the number of solutions (candidate points on the Pareto frontier) and M is the number of objective functions. Next, we proceed to the calculation of Pareto dominance, where for each point i in the dataset, we check whether there is another point j that dominates it according to the Pareto rule:

$$f_k(x_j) \leq f_k(x_i) \quad \forall k \in 1, \ldots, M, \tag{15}$$

with at least one narrow inequality. If a point i is dominated by another point j, then it is not part of the Pareto frontier. Finally, isPareto is a Boolean vector of length N, where true indicates that the point belongs to the Pareto frontier, and false indicates that the point is dominated. Each candidate point used in the Pareto front analysis corresponds to a specific configuration of the oven heating elements generated by the combinatorial script described in Section 3.1. For each configuration, the thermal model described in Section 3.2 is executed to compute the resulting heating time and total electrical energy consumption required to reach the target brick temperature. These two quantities represent the objective functions of the multi-objective optimisation problem. Therefore, each point in the objective space is defined as:

$$x_i = [E_i, t_i], \tag{16}$$

where E_i is the total electrical energy consumed and t_i is the time required to complete the heating process for configuration i. The resulting dataset forms the $N \times 2$ matrix used as input for the Pareto front computation.

4. Results and Discussion

The digital model developed in the MATLAB/Simulink® environment was tested and validated before performing optimisation analyses. In this section, the results obtained from the optimisation code are presented and discussed. The solutions identified on the Pareto front were compared with both experimental measurements and dynamic simulations.

To ensure the reliability of the optimisation outcomes, all feasible combinations were evaluated using the Simulink model. However, in the experimental campaign, only a representative subset of configurations was tested, selected based on practical constraints (e.g., time, cost, and implementation feasibility). This approach allowed experimental validation of the most significant operating points while maintaining a complete numerical verification through simulations.

4.1. Computed Heater Configurations and Associated Power Outputs

The first part of the code quickly generates all valid resistor combinations, choosing from the three installed in the oven: Grill 1700 W, Cielo 1000 W, Suola 1200 W. Table 3 shows the results of the code with the combinations and the powers associated with them.

Table 3. Heating element configurations (Grill, Cielo, Suola) and their respective power outputs. The values include series, parallel, and mixed connections, ensuring compliance with the maximum power limit of 3000 W.

Combinations	Power (W)
Grill + Suola (Parallel)	2900
Grill + Suola (Series)	703.45
Grill + Cielo (Parallel)	2700
Grill + Cielo (Series)	629.63
Suola + Cielo (Parallel)	2200
Suola + Cielo (Series)	545.45
Suola + Cielo + Grill (Series + Parallel)	2245.45
Grill + Cielo + Suola (Series + Parallel)	1829.63
Grill + Suola + Cielo (Series + Parallel)	1703.45

The results include “Series + Parallel” combinations, as well as exclusively “Parallel” or “Series” combinations. In particular, for those with three heaters, the first two are calculated in series, and the last one in parallel. As shown, no combinations exceed 3000 W, so the power constraint is correctly applied in the calculation. The code can be considered correct if its results are confirmed by manually computing the corresponding heater combinations.

4.2. Derivation of a Nonlinear Temperature Correlation from Experimental Data

This section describes the methodology used to derive the coefficients defining the correlation between the rise in brick temperature and the corresponding oven temperature. Including this correlation is essential to achieving the highest possible accuracy in the model. The correlation obtained from the code is:

$$T_{brick} = 4.8886e^{-7}T_{oven}^4 - 1.9201e{-}4T_{oven}^3 + 0.0256T_{oven}^2 - 1.329T_{oven} + 26.8664. \quad (17)$$

Figure 3 shows the comparison between the experimentally measured brick temperature and the temperature predicted by the fitted model during the heating process. The experimental data (blue markers) are in good agreement with the model predictions (red line) over the entire time interval. The model accurately reproduces the brick’s initial thermal inertia and the subsequent increase in temperature during the heating phase. The goodness-of-fit is confirmed by a coefficient of determination $R^2 = 0.97$, indicating that the model explains most of the variance in the experimental data. This agreement confirms that the proposed model can represent the changing thermal behaviour of the oven and brick system. This supports its use for the following optimisation analysis.

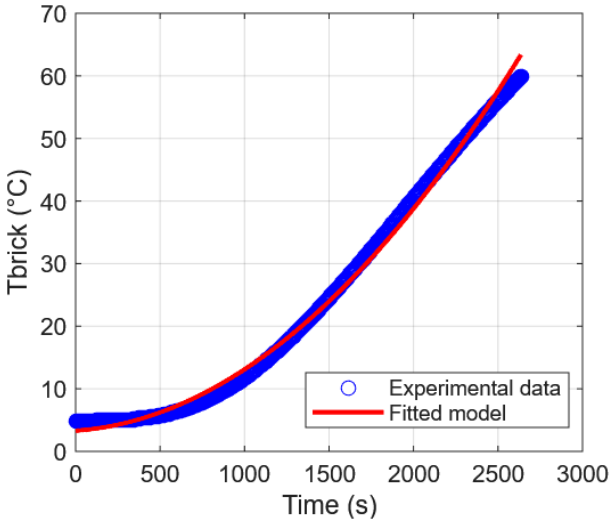

Figure 3. Results of the correlation realised in MATLAB. The red line represents the fitted model; the blue dots represent the experimental data.

4.3. Pareto Front Analysis and Validation of Optimal Energy

The specific challenge that motivated the use of optimisation models was the need to identify combinations of heating elements capable of minimising the oven's power consumption:

$$E = \int_0^{t_f} P(t)\, dt \tag{18}$$

where $P(t)$ is the instantaneous electrical power supplied to the heating elements and t_f is the final time of the heating phase. In the Pareto function created specifically for this system, described in Section 3.3, an $N \times M$ matrix was defined, where the first column represents the first dimension (energy) and the second column represents the second dimension (time). The energy and time values are extracted from the results structure generated by the previous code, and these data sets are then used to compute the Pareto front. We then extract the configurations on the Pareto front, defining *configurationspareto = results(isPareto)*. Figure 4 shows the graph of solutions on the Pareto frontier as a function of time and energy. The blue dots represent all tested configurations and, therefore, all feasible solutions to the problem. The red dots highlight the Pareto-efficient solutions—those not dominated by any other point. In other words, no alternative solution achieves lower energy consumption and shorter time simultaneously. From the distribution of points, it is evident that the Pareto-optimal solutions lie in the lower-left region of the graph, which is expected since this area corresponds to the minimum values of time and energy. All other configurations are dominated because at least one alternative performs better on at least one of the two objectives. Of all the possible configurations, the code identified three optimal points on the Pareto front. The first configuration exhibits higher energy consumption but a shorter heating time, whereas the other two configurations require more energy and longer heating times than the first. This behaviour is consistent with the Pareto front concept, which states that improving one objective necessarily degrades at least one of the others.

The Pareto front results were first evaluated using the dynamic model developed in Simulink and subsequently validated through experimental testing on the physical prototype in the laboratory. Each experimental test was repeated three times, and the reported values represent the mean ± standard deviation. Table 4 reports the energy consumption values for the three configurations selected by the optimisation code, including the results obtained from simulations and laboratory measurements, along with the corresponding

standard deviations. Additionally, the root mean square error (RMSE) between simulation and experimental results is reported to quantify the agreement between the two approaches.

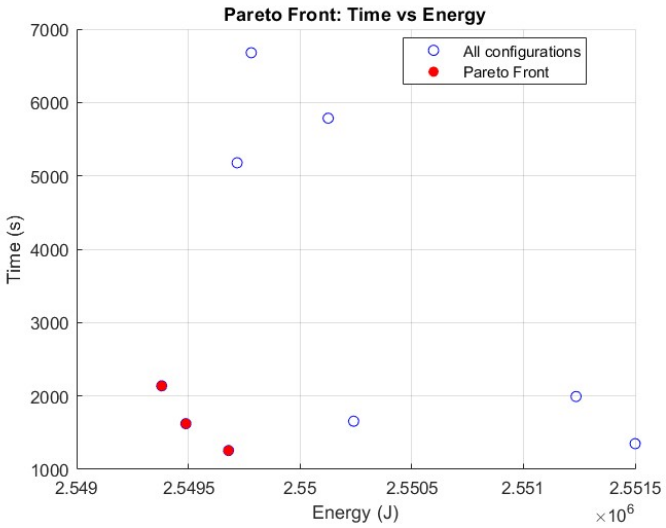

Figure 4. Pareto front distribution for multi-objective system optimisation. The x-axis shows energy in joules, while the y-axis shows time in seconds.

Table 4. Results from simulations and test.

Combinations	Code (kWh)	Simulation (kWh)	Experimental (kWh)
Grill + Suola (parallel)	1.35	1.27 ± 0.02	1.13 ± 0.03
Suola + Cielo + Grill (Series + Parallel)	1.02	1.033 ± 0.015	1.068 ± 0.02
Grill + Suola + Cielo (Series + Parallel)	0.956	0.948 ± 0.01	0.934 ± 0.015

The first row corresponds to the Parallel Grill + Suola configuration, which shows the highest energy consumption among all tested setups: 1.35 kWh in the optimisation code, 1.27 ± 0.02 kWh in the simulation, and 1.13 ± 0.03 kWh experimentally. The significant difference between the simulation and experimental results (RMSE = 0.14 kWh) likely stems from real-world factors, such as heat losses and thermal inertia, that the numerical model does not fully capture. The second row shows the Suola + Cielo + Grill (Series + Parallel) configuration. It achieves a reduction compared to the first configuration. The values are 1.02 kWh in the code, 1.033 ± 0.015 kWh in the simulation, and 1.068 ± 0.02 kWh experimentally. The smaller RMSE of 0.035 kWh shows better agreement between the simulation and experimental measurements than in the first configuration. Finally, the Grill + Suola + Cielo configuration has the lowest consumption. The code predicts 0.956 kWh, the simulation estimates 0.948 ± 0.01 kWh, and the measured value is 0.934 ± 0.015 kWh. The RMSE of 0.014 kWh confirms strong consistency between the numerical and experimental results. Overall, the comparison between the optimisation code, simulations, and laboratory experiments is shown in Figure 5. The inclusion of multiple repetitions, standard deviations, and RMSE allows for a quantitative assessment of uncertainty, confirming the reliability of the digital model in predicting real-world energy consumption.

To further assess the replicability and robustness of the optimisation code, the simulations were repeated on a different oven with a larger internal volume. The new oven has a volume of 85 L and two heating elements, in addition to the other three discussed in this work. These heating elements are called Ring, and each has a power of 1550 W. The code is designed to allow key input parameters, such as oven geometry and heating element power, to be easily modified to reflect the characteristics of a new appliance. Using these adjusted parameters, the code generated a new set of optimal configurations, which were

then evaluated through simulation and experimental tests, following the same procedure used for the oven analysed in this work. The results confirmed that the code performs consistently and accurately predicts energy consumption, with values and trends similar to those observed in the smaller oven. This approach shows that the optimisation framework can scale and adapt, enabling the same method to work across ovens of varying sizes without changing the underlying algorithms. Furthermore, the ability to quickly update input parameters ensures that the code can support future experimental setups or different appliance models, making it a reliable tool for research and practical applications. Table 5 reports the energy consumption for the same three optimal configurations when applied to both the original and the larger oven. Each experimental test was repeated three times, and the reported values represent the mean ± standard deviation. The relative difference between the two ovens is also indicated to highlight how energy consumption scales with oven size.

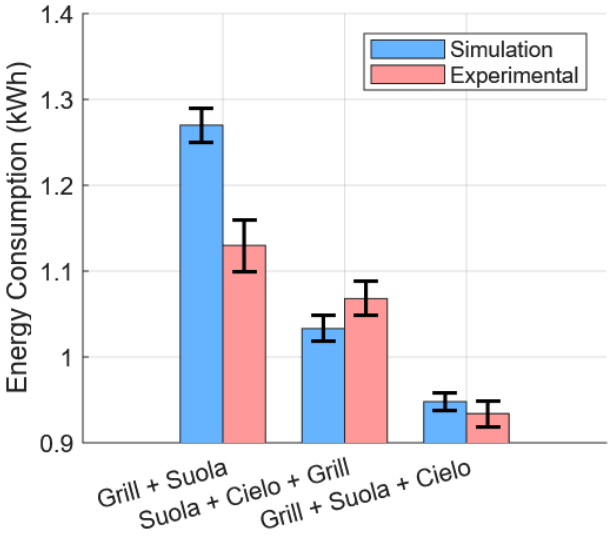

Figure 5. Comparison of energy consumption for different configurations. The blue columns show the simulation results, and the red columns represent the experimental results.

Table 5. Comparison of energy consumption between the original and larger oven for the same optimal configurations (mean ± standard deviation). Relative difference indicates percentage change.

Configuration	70 L (kWh)	85 L (kWh)	Simulation Std (kWh)	Experimental Std (kWh)	Relative Difference (%)
Grill + Suola (Parallel)	1.27	1.48	0.02	0.03	+16.5%
Suola + Cielo + Grill (Series + Parallel)	1.033	1.20	0.015	0.02	+16.2%
Grill + Suola + Cielo (Series + Parallel)	0.948	1.11	0.01	0.015	+17.1%

As expected, the larger oven exhibits higher energy consumption, with an increase of 16–17% across all configurations. Despite this, the relative ranking of the configurations remains unchanged, confirming that the optimisation code is robust and its recommendations are consistent and scalable. These results demonstrate that, by modifying only the input parameters—such as oven volume, heater positions, and thermal properties—the code can reliably predict optimal configurations for different appliances. This confirms both the replicability and the general applicability of the optimisation methodology across ovens of different sizes.

5. Conclusions

In this work, a new optimisation approach for domestic ovens was presented. It aims to manage the heating elements efficiently to reduce both energy use and heating time. The optimisation code was developed in MATLAB®, while the oven's digital model was created in Simulink®. The goal was to find configurations that strike the best balance between lowering electrical energy and shortening heating duration. The effectiveness of this approach was confirmed through simulations and experimental tests. The configurations identified by the optimisation algorithm continually provide the best compromise between energy use and heating time, taking into account the specific characteristics of the oven studied. These results highlight the increasing importance of digital tools and model-based methods in supporting traditional experimental testing. The implemented workflow generates all possible heater combinations before choosing the most effective solutions. This gives a significant advantage when analysing the full range of electromechanical oven models. Due to its adaptability, the method can be applied to ovens with various designs, heating element configurations, and internal volumes, making it a flexible tool for broader design and optimisation frameworks. Lastly, even for a relatively simple system like a domestic oven, Pareto front analysis proves very valuable. It helps designers see and choose configurations that balance the goals of reducing energy and time. By showing the full range of optimal trade-offs, the Pareto front allows for more informed and flexible design decisions. It highlights options that may not be clear from focusing on a single objective.

Author Contributions: Conceptualisation, S.R.; methodology, S.R.; software, S.R.; validation, S.R. and B.B.P.; formal analysis, S.R.; investigation, S.R.; resources, B.B.P. and M.R.; data curation, S.R.; writing—original draft preparation, S.R.; writing—review and editing, S.R.; supervision, B.B.P. and M.R.; project administration, B.B.P.; funding acquisition, M.R. All authors have read and agreed to the published version of the manuscript.

Funding: This research received no external funding.

Data Availability Statement: The original contributions presented in this study are included in the article. Further inquiries can be directed to the corresponding author.

Acknowledgments: The authors would like to thank all SMEG employees who helped with the instruments during the tests in their workshops.

Conflicts of Interest: Author Marco Reguzzoni was employed by the company Research and Development Department, SMEG S.p.A. The remaining authors declare that the research was conducted in the absence of any commercial or financial relationships that could be construed as a potential conflict of interest. The company had no role in the design of the study; in the collection, analyses, or interpretation of data; in the writing of the manuscript, or in the decision to publish the results.

Abbreviations

The following abbreviations are used in this manuscript:

MOO	Multi-Objective Optimisation
MO	Multi-Objective
DM	Decision Maker
NSGA-II	Non-dominated Sorting Genetic Algorithm
MOEA/D	Multi-Objective Evolutionary Algorithm based on Decomposition
CFD	Computational Fluid Dynamics

References

1. Tanya, G.; Adedeji, A.; Ngadi, M.; Raghavan, V. Drying Characteristics of Pulsed Electric Field-Treated Carrot. *Dry. Technol.* **2008**, *26*, 1244–1250. [CrossRef]
2. Russo, M.; Serra, D.; Suraci, F.; Di Sanzo, R.; Fuda, S.; Postorino, S. The potential of e-nose aroma profiling for identifying the geographical origin of licorice (*Glycyrrhiza glabra* L.) roots. *Food Chem.* **2014**, *165*, 467–474. [CrossRef]
3. Khatir, Z.; Paton, J.; Thompson, H.; Kapur, N.; Toropov, V.; Lawes, M.; Kirk, D. Computational Fluid Dynamics (CFD) investigations of air flow and temperature distribution in a small scale bread-baking oven. *Appl. Energy* **2012**, *89*, 89–96. [CrossRef]
4. Papasidero, D.; Corbetta, M.; Pierucci, S.; Pirola, C.; Manenti, F. Studying Oven Technology towards the Energy Consumption Optimisation for the Baking Process. *Chem. Eng. Trans.* **2015**, *45*, 481–486. [CrossRef]
5. Monde, A.; Cannistraro, M. Design and control intended low-order model for transient investigation of an electric oven: Static mode. *Int. J. Heat Mass Transf.* **2024**, *221*, 125061. [CrossRef]
6. Ramirez-Laboreo, E.; Sagues, C.; Llorente, S. Dynamic heat and mass transfer model of an electric oven for energy analysis. *Appl. Therm. Eng.* **2016**, *93*, 683–691. [CrossRef]
7. Suzzi, N.; Lucchi, M.; Lorenzini, M. Dynamic Model for Convective Heating of a Wet Brick during Energy Characterisation of Domestic Electric Ovens. *Appl. Therm. Eng.* **2019**, *161*, 114117. [CrossRef]
8. *EN 60350-1*; Household Electric Cooking Appliances—Part 1: Ranges, Ovens, Steam Ovens and Grills—Methods for Measuring Performance. International Electrotechnical Commission: Geneva, Switzerland, 2023.
9. Ureta, M.; Goñi, S.; Salvadori, V.; Olivera, D. Energy requirements during sponge cake baking: Experimental and simulated approach. *Appl. Therm. Eng.* **2016**, *115*, 637–643. [CrossRef]
10. Park, D.; Seo, E.; Kwon, M.; Park, Y. The study on the heater usage for better energy efficiency of domestic convection oven. *J. Mech. Sci. Technol.* **2018**, *32*, 907–914. [CrossRef]
11. Mindeel, T.; Spentzou, E.E.; Eftekhari, M. Energy, thermal comfort, and indoor air quality: Multi-objective optimization review. *Renew. Sustain. Energy Rev.* **2024**, *202*, 114682. [CrossRef]
12. Taghavi, M.; Ferrantelli, A.; Joronen, T. Multi-objective optimization of a plate heat exchanger thermal energy storage with phase change material. *J. Energy Storage* **2024**, *89*, 111645. [CrossRef]
13. Pereira, J.L.; Oliver, G.; Francisco, M.; Cunha, S., Jr.; Gomes, G. A Review of Multi-objective Optimization: Methods and Algorithms in Mechanical Engineering Problems. *Arch. Comput. Methods Eng.* **2021**, *29*, 2285–2308. [CrossRef]
14. Kuroda, K.; Magori, H.; Ichimura, T.; Yokoyama, R. A hybrid multi-objective optimization method considering optimization problems in power distribution systems. *J. Mod. Power Syst. Clean Energy* **2015**, *3*, 41–50. [CrossRef]
15. Goñi, S.M.; Salvadori, V.O. Model-based multi-objective optimization of beef roasting. *J. Food Eng.* **2012**, *111*, 92–101. [CrossRef]
16. Khatir, Z.; Taherkhani, A.; Paton, J.; Thompson, H.; Kapur, N.; Toropov, V. Energy thermal management in commercial bread-baking using a multi-objective optimisation framework. *Appl. Therm. Eng.* **2015**, *80*, 141–149. [CrossRef]
17. Zhang, M. Multi-Objective Optimal Reactive Power Dispatch of Power Systems by Combining Classification-Based Multi-Objective Evolutionary Algorithm and Integrated Decision Making. *IEEE Access* **2020**, *8*, 38198–38209. [CrossRef]
18. Martins, P.; Oleskovicz, M. Multi-Objective Optimization Aiming to Minimize the Number of Power Quality Monitors and Multiple Fault Estimations in Unbalanced Power Distribution Systems. *IEEE Trans. Power Deliv.* **2021**, *37*, 1315–1323. [CrossRef]
19. Ma, Z.; Zhu, A.; Feng, H.; Zhou, C.; Liu, H.; Sheng, D.; Guo, H.; Su, C. Research on path and energy consumption control of six-axis manipulator based on multi-objective optimization method. *Int. Sci. Tech. Econ. Res.* **2025**, *8*, 96–113.
20. Giagkiozis, I.; Fleming, P. Pareto Front Estimation for Decision Making. *Evol. Comput.* **2014**, *22*, 651–678. [CrossRef] [PubMed]
21. Sharma, S.; Chahar, V. A Comprehensive Review on Multi-objective Optimization Techniques: Past, Present and Future. *Arch. Comput. Methods Eng.* **2022**, *29*, 5605–5633. [CrossRef]
22. Kang, S.; Li, K.; Wang, R. A survey on pareto front learning for multi-objective optimization. *J. Membr. Comput.* **2024**, *7*, 128–134. [CrossRef]
23. Asrari, A.; Lotfifard, S.; Payam, M.S. Pareto Dominance-Based Multiobjective Optimization Method for Distribution Network Reconfiguration. *IEEE Trans. Smart Grid* **2016**, *7*, 1401–1410. [CrossRef]
24. Rustico, S.; Pulvirenti, B.; Useli, G.; Reguzzoni, M. Multi-Level Simulation for Dynamic Analysis of A Domestic Electric oven in Forced Convective Heating—Evaluation and Optimization of Energy Consumption Using the Brick Test. *Future Cities Environ.* **2025**, *11*, 15–27. [CrossRef]
25. Mistry, H.; Ganapathisubbu, S.; Dey, S.; Bishnoi, P.; Castillo, J.L. A methodology to model flow-thermals inside a domestic gas oven. *Appl. Therm. Eng.* **2011**, *31*, 103–111. [CrossRef]
26. Mistry, H.; Ganapathi-subbu; Dey, S.; Bishnoi, P.; Castillo, J.L. Modeling of transient natural convection heat transfer in electric ovens. *Appl. Therm. Eng.* **2006**, *26*, 2448–2456. [CrossRef]
27. Rek, Z.; Rudolf, M.; Zun, I. Application of CFD Simulation in the Development of a New Generation Heating Oven. *Stroj. Vestn.—J. Mech. Eng.* **2012**, *58*, 134–144. [CrossRef]

28. *IEC 60335-2-6:2022*; Household and Similar Electrical Appliances—Safety—Part 2–6: Particular Requirements for Stationary Cooking Ranges, Hobs, Ovens and Similar Appliances. International Electrotechnical Commission: Geneva, Switzerland, 2022. Available online: https://webstore.iec.ch/publication/99834 (accessed on 23 February 2025).
29. Garcia Asuero, A.; Sayago, A.; González, G. The Correlation Coefficient: An Overview. *Crit. Rev. Anal. Chem.* **2006**, *36*, 41–59. [CrossRef]
30. Ngatchou, P.N.; Zarei, A.; Fox, W.L.J.; El-Sharkawi, M.A. Pareto Multiobjective Optimization. In *Modern Heuristic Optimization Techniques*; Wiley: Hoboken, NJ, USA, 2007; pp. 189–207. [CrossRef]
31. Coello, C.; Van Veldhuizen, D.; Lamont, G. *Evolutionary Algorithms for Solving Multi-Objective Problems*, 2nd ed.; Springer: New York, NY, USA, 2007. [CrossRef]
32. MathWorks. gamultiobj. Available online: https://mathworks.com/help/gads/gamultiobj.html (accessed on 23 February 2025).